Evaluation of the Performance of GNSS Antennas and Modules for Electronic Navigation Seals under Challenging Operating Conditions

Altay Aitmagambetov
International Information Technology University, Almaty, Kazakhstan
a.aitmagambetov@edu.iitu.kz

Sabyrzhan Zhumagali
Institute of Space Technique and Technology, Almaty, Kazakhstan
zhumagali.s@istt.kz

Aigul Kulakayeva
International Information Technology University, Almaty, Kazakhstan
a.kulakayeva@iitu.edu.kz (corresponding author)

Leila Sultanbekova
Institute of Space Technique and Technology, Almaty, Kazakhstan
sultanbekova.l@istt.kz

Anatoly Samsonenko
Institute of Space Technique and Technology, Almaty, Kazakhstan
samsonenko.a@istt.kz

Received: 30 September 2025 | Revised: 28 October 2025 | Accepted: 3 November 2025

Licensed under a CC-BY 4.0 license | Copyright (c) by the authors | *DOI: https://doi.org/10.48084/etasr.15226*

ABSTRACT

This study focuses on the experimental selection of the optimal Global Navigation Satellite System (GNSS) antenna for integration into a domestically developed navigation seal designed for transport logistics and digital customs control tasks in the Republic of Kazakhstan. The relevance of this study stems from the need to enhance technological independence and improve cargo monitoring efficiency to support domestic manufacturing and technological self-reliance. The scientific novelty lies in a comprehensive comparative assessment of commercial antennas not only in laboratory settings but also under field conditions, including installation on metallic surfaces, which reflects real operational scenarios. The objective of the research is to select an antenna that ensures the best balance between cost and performance for integration into the locally developed navigation seal. To achieve this, laboratory measurements and field experiments were conducted, analyzing parameters such as cold start time, carrier-to-noise density ratio (C/N_0, dB-Hz) for each satellite, the number of visible and used satellites, accuracy indicators (Position Dilution of Precision (PDOP), Horizontal Dilution of Precision (HDOP), Vertical Dilution of Precision (VDOP)), and tracking stability under internal and external shielding effects. As a result, the 1575R-A antenna was identified as having the most favorable characteristics among the tested samples and can be recommended for integration into the developed navigation seal. The practical significance of the study lies in providing recommendations for local manufacturers, whereas its theoretical contribution is the expansion of knowledge on the impact of structural and operational factors on the efficiency of GNSS antennas in compact devices.

Keywords-Electronic Navigation Seal (ENS); GNSS antennas; cold-start TTFF; multipath mitigation

I. INTRODUCTION

In recent years, the development of Electronic Navigation Seals (ENSs) has gained increasing importance due to the growing demand for reliable cargo tracking, digital customs control, and transparency in supply chains. These devices, based on Global Navigation Satellite System (GNSS) technologies, play a crucial role in the continuous and secure monitoring of container movements, particularly in cross-border transportation.

The Republic of Kazakhstan, with its strategic position as a transit country on the Eurasian transport corridor and active participation in initiatives such as the Belt and Road, is facing a growing demand for the implementation of modern navigation seals. However, the widespread use of foreign ENSs is associated with several limitations, including high procurement costs, dependence on external suppliers, insufficient adaptation to local technical requirements, and challenges in maintenance and certification.

Currently, the domestic market offers virtually no accessible and technically optimized navigation seal solutions that are fully developed and manufactured in the Republic of Kazakhstan. This highlights the need for an in-house engineering design that considers real operating conditions, such as the presence of metallic surfaces during installation, exposure to temperature and climatic factors, as well as cost constraints for large-scale implementation.

ENSs are an integral component of digital logistics, combining GNSS positioning, wireless communication (GSM/LTE/NB-IoT), telemetry, and tamper detection functions to ensure continuous container monitoring. Their functional and operational requirements are defined by the international ISO 18185 series of standards, which regulate equipment identification, integrity, and interoperability [1-3].

GNSS technology has been in use for more than four decades [4], and continuous advancements have improved positioning accuracy from the meter level to the sub-centimeter level, meeting the demand for high-precision navigation in engineering, transportation, and geodetic applications. However, the cost of high-quality geodetic receivers remains high, prompting researchers to consider low-cost GNSS receivers as a viable alternative [5]. Current trends indicate that the development of affordable multi-frequency receivers will further promote the widespread adoption of GNSS technologies across various industries [6, 7].

One of the key engineering challenges in the miniaturization of ENSs is ensuring stable GNSS signal reception in the presence of nearby metallic structures, such as container walls or locking mechanism components. The metallic environment can significantly alter the radiation pattern, gain, and impedance matching of the antenna, as well as increase the risk of detuning and multipath effects. Several studies confirm that the size and configuration of the ground plane, as well as the feeding method of the antenna, play a decisive role in shaping its electrical characteristics.

Theoretical and applied studies on microstrip and patch antennas demonstrate that ground-plane parameters directly affect the operating bandwidth, Voltage Standing Wave Ratio (VSWR), gain, and beamwidth. For ceramic L1 patches, optimal results are typically achieved with a limited ground plane of approximately 50–70 mm in diameter; however, such designs remain sensitive to the antenna's geometry and feed point [8]. Manufacturer guidelines (Tallysman, Taoglas) and experimental studies confirm that increasing the size or altering the shape of an additional ground plane beneath the antenna can improve gain and positioning accuracy, but may also shift the resonant frequency, requiring retuning [9, 10]. In the development of GNSS modules for compact Internet of Things (IoT) devices, including ENS, the impact of nearby metallic and dielectric elements on antenna performance is specifically emphasized. These factors necessitate a compromise between the dimensional constraints of the design and the required radio-frequency characteristics [11].

In environments with closely spaced metallic objects and in dense urban areas, multipath propagation becomes one of the main factors degrading GNSS navigation accuracy. Signals reflected from surfaces distort the receiver's correlation function, cause pseudorange biases, and deteriorate the quality of the navigation solution. For instance, authors in [12] proposed a local filtering method that accounts for the spatial correlation of errors, thereby improving the accuracy of relative positioning in high-precision applications. In [13], it was demonstrated that antenna arrays and beamforming algorithms can significantly mitigate the effects of reflected signals compared to single-antenna configurations. In [14], it is emphasized that traditional correlation methods are less effective against short-path, high-amplitude reflections, and a combination of antenna array signal processing with local least-squares filtering is recommended. Additionally, authors in [15] explored the use of metasurfaces for decoupling and shielding closely spaced antenna elements, which improves the radiation pattern and reduces mutual interference in compact GNSS arrays. Collectively, these studies confirm that robust multipath mitigation in compact, enclosure-constrained GNSS systems requires a comprehensive approach that integrates spatial filtering and antenna array techniques with innovative structural solutions, such as metasurface integration. A recent study [16] further demonstrated that integrated dual-antenna designs on a single ground plane can effectively cover multiple satellite communication bands (L- and S-bands) while maintaining low VSWR, high gain, and broad beamwidth, which is particularly relevant for compact ENS modules operating under spatial and material constraints.

Methodologies for testing GNSS antennas and modules are generally divided into two main approaches: laboratory measurements (S-parameters, Amplitude–Frequency Response (AFR), or transfer function S21 in an Anechoic Chamber (AC)) and field tests (determination of cold-start Time to First Fix (TTFF), satellite signal-to-noise ratio, and Dilution of Precision (DOP) metrics). S21 measurement in an AC using reference sources and receivers is recognized as a valid method for comparing gain and frequency selectivity, provided that proper path calibration and the influence of connecting cables are controlled [17]. However, for the form factor of a navigation seal, it is crucial to simulate and verify characteristics specifically under "on-metal" installation conditions and within

the enclosure, as free-space results often yield overestimated performance. Studies have documented cases of detuning and efficiency degradation when antennas are positioned close to metallic or dielectric surfaces [18].

Additionally, authors in [19] showed that near-field interference can affect high-precision positioning results. In particular, the antenna installation method during an observation campaign, including its distance from other antennas, can introduce biases of up to 3 mm in the vertical component of pseudo-kinematic solutions. The dispersion of results increases when an additional object is located in the near-field region of the measurement antenna, intersecting its radiation pattern, both for GPS and combined GPS/GLONASS scenarios.

In [20], using the Hannover's Automated Absolute Antenna Field Calibration Technique developed by the Institut für Erdmessung, Universität Hannover, and Geo, it was demonstrated that mechanical elements beneath the antenna can cause significant variations in the phase center offset and Phase Center Variations (PCV), described by spherical harmonic models. For GPS L1 and L2 signals, changes in differential PCV (DPCV) reach several millimeters, and long-term static observations do not eliminate this systematic error but instead introduce a persistent bias into coordinate estimation.

The key operational parameters of GNSS receivers include cold-start time (TTFF), fix stability (FIX), sensitivity, and satellite constellation geometry metrics (Position Dilution of Precision (PDOP), Horizontal Dilution of Precision (HDOP), Vertical Dilution of Precision (VDOP)). TTFF is defined as the time from powering on the device to obtaining the first valid solution and depends on the availability of almanac and ephemeris data [21]. PDOP, HDOP, and VDOP indicators reflect the quality of satellite geometry: the lower the DOP value, the higher the potential positioning accuracy. Common definitions and analytical approaches for evaluating these parameters are well established in studies [22, 23]. Assisted GNSS (A-GNSS) technologies significantly reduce TTFF, which is particularly important in challenging reception environments [24]. A comparative analysis conducted in [25] showed that among the four global systems, GPS provides the lowest TTFF and the highest reliability under cold-start conditions, whereas GLONASS, BeiDou, and Galileo exhibit higher start times or lower accuracy.

The modern selection of GNSS modules for ENS is based on a balance between sensitivity, power consumption, and size. For instance, the u-blox M10 platform supports simultaneous reception of four systems with low power consumption, making it attractive for autonomous devices, whereas the earlier M8 series remains a widely adopted and reliable solution for industrial applications [26-28]. In this case, the choice of hardware platform is determined not only by positioning performance but also by operating conditions, power supply architecture, and integration requirements for enclosure-constrained designs.

In the future, algorithmic approaches to improving communication robustness [29] and the implementation of modern networking solutions to increase data transmission capacity and reliability [30] can also be considered.

Nevertheless, for the Republic of Kazakhstan, which is actively developing its transport and logistics infrastructure and digital customs control, the adaptation of antennas to real operating conditions, including installation on container metallic surfaces, remains a critical issue. The lack of such studies limits the ability of domestic developers to select optimal solutions capable of ensuring reliable positioning at an acceptable cost. Therefore, this study aims to address this gap by identifying an antenna suitable for integration into a nationally developed navigation seal.

The central research question of this study is as follows: to what extent can cost-effective commercial GNSS antennas and modules ensure reliable performance when integrated into the design of a domestically developed navigation seal intended for operation in the specific conditions of the Republic of Kazakhstan?

The working hypothesis of this study assumes that, with proper selection and experimental verification, it is possible to achieve performance characteristics comparable to industrial solutions, even under resource-constrained conditions.

To test this hypothesis, a structural prototype of a domestically produced navigation seal was designed and assembled using 3D printing and a modular approach. The study involved a two-stage testing process: laboratory measurements of antenna AFRs (S21) in an AC, and field tests that included evaluating cold-start time, the number of visible satellites, carrier-to-noise density ratio (C/N_0) for each satellite, as well as positioning accuracy parameters (PDOP, HDOP, VDOP) under conditions close to real-world operation.

The results of this study support the initiative to develop an optimized navigation seal that can be manufactured in the Republic of Kazakhstan, with subsequent certification and scalable integration into the country's logistics chains.

II. MATERIALS AND METHODS

This study included both laboratory bench testing and comprehensive field evaluation of four active ceramic GNSS antennas (1575R-A, Plosk, Uz, Uzk) and six GNSS modules (u-blox MAX M10S, MAX M8Q, Quectel L76KB, ATGM336H, Neoway Q7A, SIM868) for integration into the navigation seal under development. In the field tests of the antennas, all of them were connected to the u-blox ZTD-F9P module. In the module performance tests, a single 1575R-A antenna was used for all modules.

For comparative analysis, the u-blox W1220AS antenna model was used as a reference sample, distinguished by its high gain and frequency selectivity at GPS and GLONASS frequencies. However, the high cost of the W1220AS makes it economically impractical for large-scale production of serial navigation seals. Nevertheless, its characteristics allow this antenna to serve as a reference sample, providing an objective benchmark for evaluating the performance of more affordable antenna solutions intended for practical implementation.

To conduct the experimental evaluation of GNSS antennas and communication modules, a structural sketch of the developed navigation seal was designed, as shown in Figure 1.

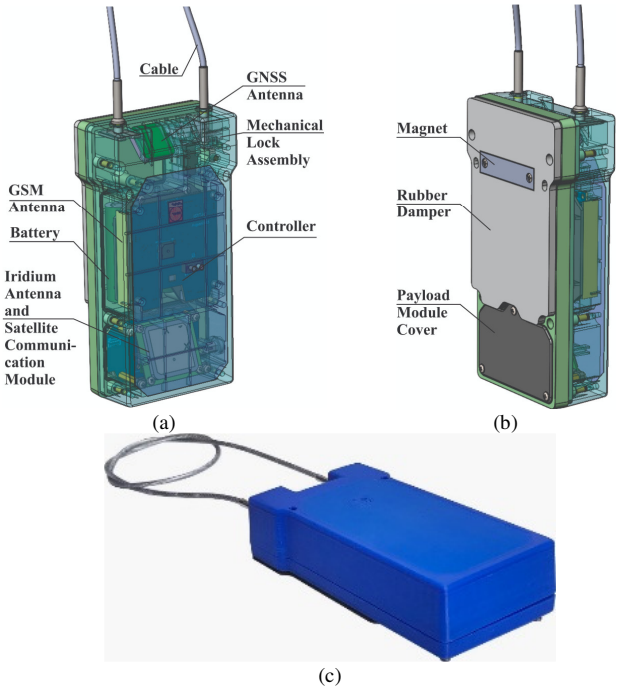

Fig. 1. Layout of the navigation seal components and modules: (a) internal structure, (b) assembled configuration, and (c) 3D-printed prototype.

Based on this design, a plastic housing of the device was fabricated using 3D printing technology (Figure 1(c)), followed by the assembly of the experimental prototype with the integration of antenna modules, battery, controller, and other components in accordance with the project layout. Figure 1 shows the main functional elements of the of the developed navigation seal: antenna modules, battery, controller, mechanical locking unit, and payload components. The specific features of this configuration were carefully considered during laboratory and field tests to ensure that the testing conditions closely approximated real-world operation.

In terms of structural parameters, PA12+GF plastic is the most suitable choice for the navigation seal. It meets the operational requirements, including resistance to chemical de-icing agents, petroleum products, impact loads from stones and accidental drops, as well as temperature fluctuations typical of a sharply continental climate. PA12+GF is a composite material and a type of nylon reinforced with glass fiber (up to 30%). Due to the addition of glass fiber, the material demonstrates improved resistance to mechanical loads and deformation.

Its resistance to Ultraviolet (UV) exposure is moderate compared to other plastics considered in the project (ABS, PLA, PETG, and PA12). The addition of UV stabilizers improves UV resistance; however, such additives reduce radio transparency, whereas the presence of glass fiber increases the dielectric constant $\varepsilon_{PA12+GF}$ to 3.5–4.5. For comparison, the dielectric constant of ABS (ε_{ABS}) is approximately 2.8–3.2.

To minimize the influence of the material's dielectric constant on antenna performance, an air gap of 1.5–2 mm was provided between the enclosure wall and the ceramic antenna element, achieved through small structural protrusions and dedicated mounting seats. To maintain an acceptable level of radio transparency (comparable to ABS), the wall thickness in the antenna installation areas was reduced from 3.5 mm to 2 mm, forming radio-transparent windows. An important criterion when selecting the material for mass production is the possibility of hot injection molding. PA12+GF enables manufacturing of the enclosure both through 3D printing and injection molding.

Figure 2 illustrates the block diagram of the developed navigation seal, which consists of three main modules: an electromechanical module that ensures the integrity control of the sealing element and provides physical protection of the device; a processing module responsible for handling navigation and diagnostic data, as well as managing the communication subsystems, including the GSM antenna; and a payload module, into which additional sensors may be integrated.

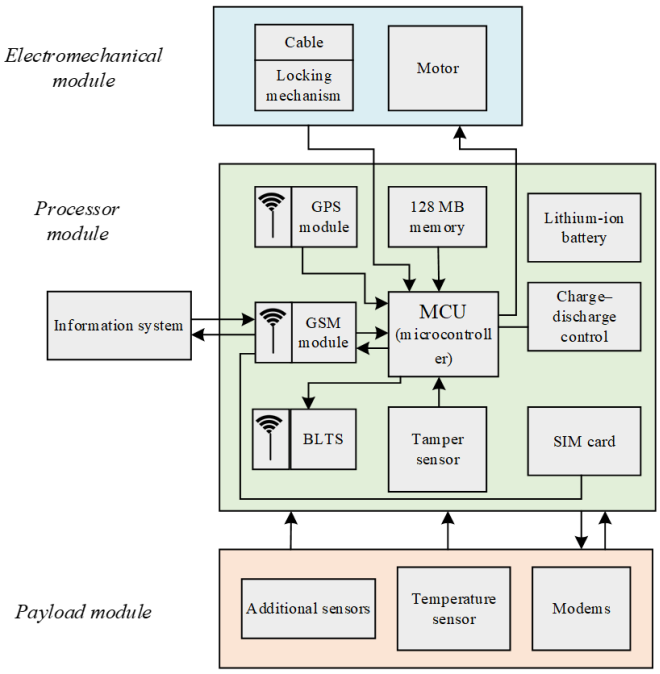

Fig. 2. Structural diagram of the modular navigation seal.

Manufacturers of navigation seals typically aim to develop non-serviceable, non-disassemblable designs with a minimal number of covers and screws to ensure maximum protection and reliability. The introduction of a modular architecture may reduce structural robustness; however, the added functionality—including a backup satellite communication channel and the ability to switch individual modules to sleep mode depending on operational requirements and system status—is expected to significantly extend the autonomous

operating time of the navigation seal. For antenna parameter measurements at the laboratory stage, a test bench was used consisting of a Keysight FieldFox N9915A vector network analyzer, a test helical antenna mounted in a conical reflector, a bias tee, a +3 V laboratory power supply, and a Huber+Suhner RF cable (Figure 3). Experimental measurements were carried out in the shielded AC of the Institute of Space Technique and Technology (ISTT).

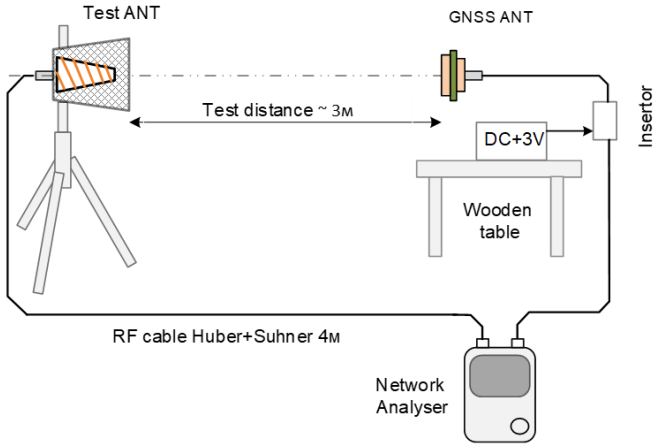

Fig. 3. Measurement setup for the GNSS antenna frequency response in the AC of ISTT.

The AFR (S21) measurements were carried out at a distance of 3 m using a broadband helical antenna mounted in a conical reflector as the test antenna. The built-in low-noise amplifiers of the tested antennas were powered through the cable via a bias-tee from a laboratory power supply (+3 V), in accordance with the antenna manufacturers' datasheets (Figure 4). As a result, the AFRs of the GNSS antennas were obtained, enabling the assessment of frequency selectivity and gain relative to the reference (benchmark) u-blox W1220AS antenna, as well as the influence of the dielectric properties of the plastic enclosure on the AFR. The selectivity and gain parameters of the W1220AS antenna are close to the best industry standards, which makes it suitable for use as a reference sample for comparative evaluation of the effectiveness of more cost-efficient antenna solutions intended for mass-produced devices.

The navigation seal enclosure at the GNSS antenna installation area was intentionally designed with a 45° tilt, as shown in Figure 4(b), to prevent snow and ice accumulation on the surface during the cold season. Snow and ice buildup may lead to signal attenuation or even complete signal loss. Other areas of the enclosure contain multiple metal components, which are also unfavorable for stable antenna performance.

The ABS enclosure does not feature such an inclined surface, and the GNSS antennas were positioned perpendicular to the radiation of the test antenna during the S21 measurements in the AC. To ensure equal measurement conditions for the antennas placed in the PA12+GF enclosure, the navigation seal was tilted at the same angle during the measurements, as shown in Figures 4(c) and 4(d).

(a)

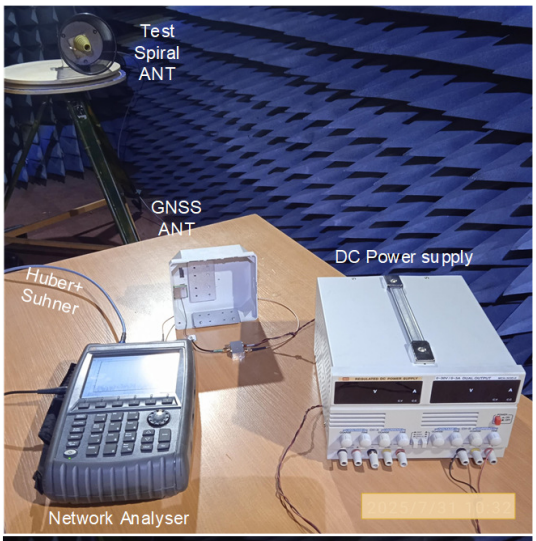

(b)

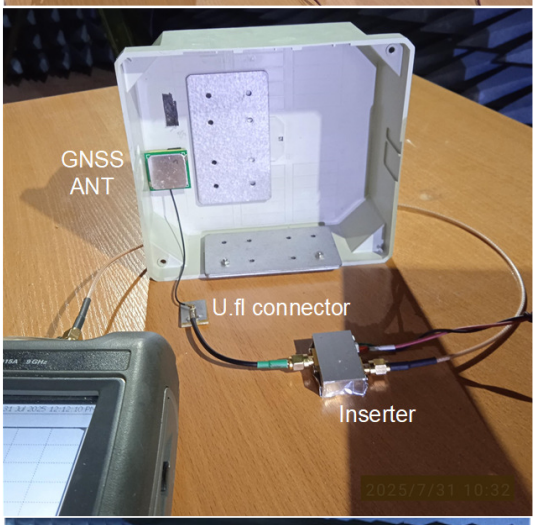

(c)

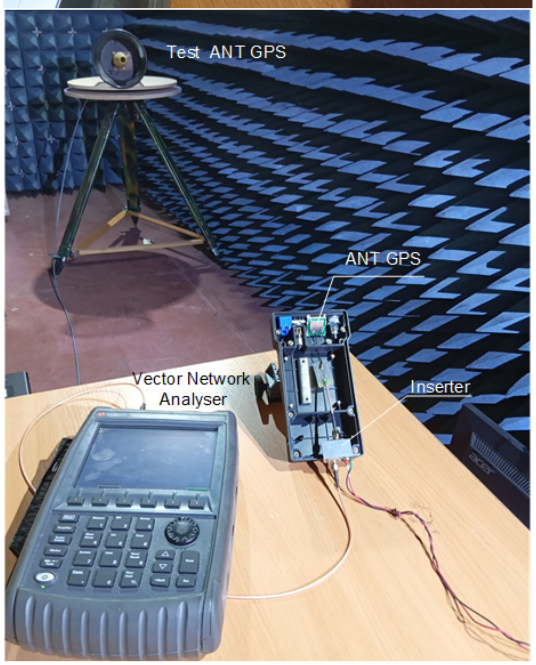

(d)

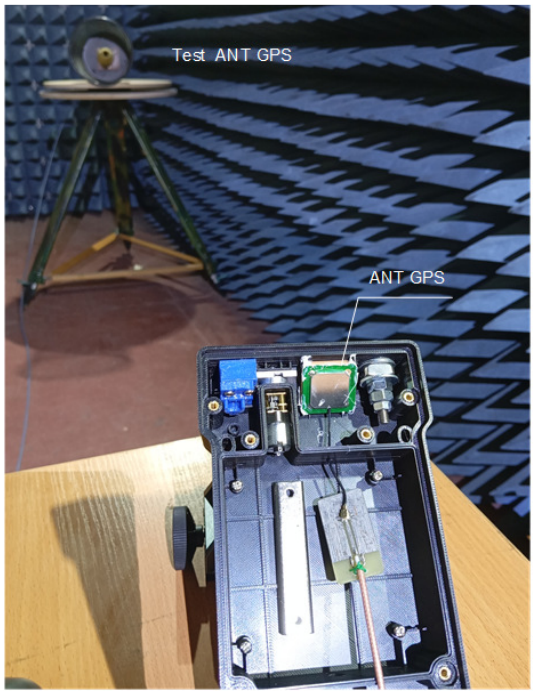

Fig. 4. Photographs of the laboratory test bench for GNSS antenna measurements in the AC of ISTT: (a) general view of the measurement setup, (b) GNSS antenna with ABS enclosure and bias-tee, (c) measurement setup with the PA12+GF enclosure, and (d) GNSS antenna with PA12+GF enclosure.

The subsequent stages of testing were conducted in the field. The antennas were sequentially tested in combination with the GNSS module under open-field conditions with the maximum possible number of visible satellites (GPS + GLONASS) to objectively evaluate sensitivity and determine the potential performance of each antenna.

The collection and synchronization of experimental data, as well as the management of cold-start scenarios, were performed using a dedicated Python-based software developed by the specialists of the ISTT. The warm-start time was 2–3 s for all modules tested with different antennas. The GNSS antennas were then mounted inside the fabricated navigation seal enclosure at a 45° angle to the horizon, in accordance with the enclosure design.

To evaluate the influence of internal layout on antenna parameters, additional mock-ups of the navigation seal's plastic enclosure were used, incorporating different configurations of metallic and electronic components. This stage was implemented using a portable field test stand comprising a laptop equipped with a dedicated interface program, an external GNSS receiver module, and the antenna installed inside the navigation seal enclosure. To reproduce conditions representative of real operation, a laminated metal sheet was used to simulate the wall of a transport container, ensuring that the influence of conductive surfaces on antenna performance could be accurately assessed. This setup enabled an objective assessment of the impact of nearby metallic objects on signal reception quality. A visual representation of the experimental setup is provided in Figure 5.

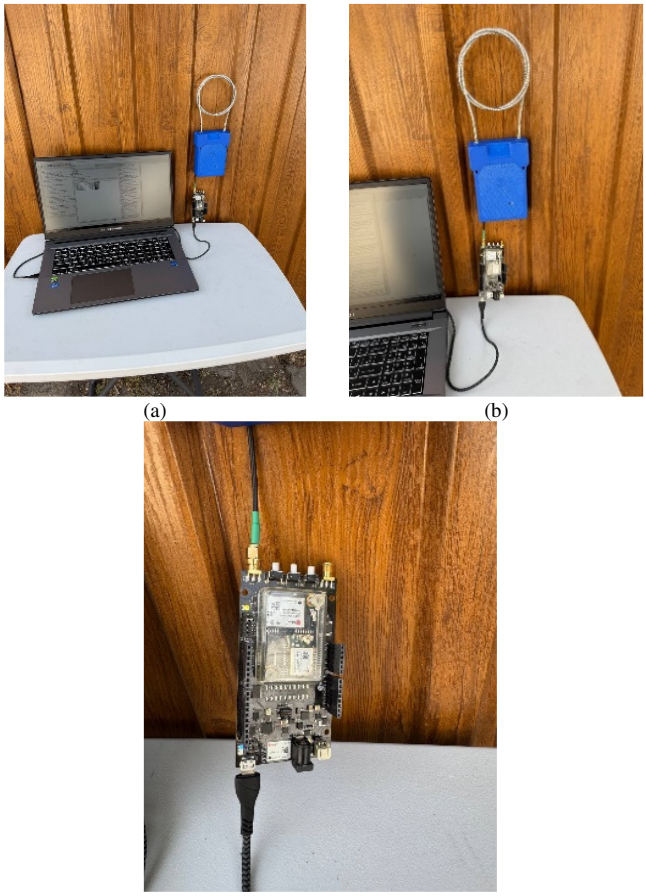

(a) (b) (c)

Fig. 5. Field test stand for GNSS antenna outdoor trials: (a) general view of the portable test setup, (b) external GNSS receiver module, and (c) GNSS receiver adapter.

The use of GPS-only signals in the second stage is due to the fact that, in most practical scenarios, GNSS receivers are primarily oriented towards the GPS constellation, whereas GLONASS is typically employed as an auxiliary system to refine positioning. In all cases, testing was carried out with reference to the benchmark antenna W1220AS.

For each antenna, the cold-start TTFF (from power-on to the first coordinate fix), the number of visible satellites, and the C/N_0 values for each satellite were recorded, taking into account the AFR of the antennas. When comparing the GNSS modules, parameters such as sensitivity, cold-start time, and power consumption (tracking mode current) were evaluated. Additionally, the performance of the modules under various backup power configurations was tested to analyze their capability for rapid position recovery after exiting sleep mode.

The key criteria for evaluating the antennas included sensitivity level, matching quality with the navigation module, signal reception stability within the navigation seal enclosure, start-up time, as well as resistance to external operating conditions and the structural characteristics of the enclosure. For GNSS modules, power consumption, positioning accuracy, and stability, as well as operational features under mass-production conditions, were considered.

III. RESULTS

A. Comparative Analysis of GNSS Module Characteristics

Table I presents the main technical specifications of six widely used GNSS modules selected for subsequent experimental testing. The comparison is based on data obtained from publicly available manufacturer technical specifications.

The comparative analysis showed that the overall dimensions of the presented GNSS modules range from 10.1 × 9.7 × 2.2 mm to 17.6 × 15.7 × 2.3 mm. All modules support the GPS navigation system. Additional systems, such as GLONASS, BeiDou, Galileo, and QZSS, are implemented in various combinations depending on the model. The sensitivity values specified in the technical documentation range from –160 to –167 dBm. Cold-start times vary from 24 to 32 s, and the declared tracking mode current consumption ranges from 6.8 to 28 mA. The UART interface is implemented in all modules, whereas Inter-Integrated Circuit (I²C) and Serial Peripheral Interface (SPI) are available only in selected models. All the presented data were obtained from publicly available manufacturer specifications and were used at the preliminary selection stage for subsequent testing.

Most of the tested modules are also equipped with a V_BCKUP (or V_BAT) pin, which ensures the preservation of ephemeris and almanac data between sessions, thereby reducing both power consumption and start-up time.

TABLE I. COMPARATIVE CHARACTERISTICS OF GNSS MODULES

Module	u-blox MAX M10S	u-blox MAX M8Q	Quectel L76KB-A58	ATGM336H (5N31/6N-74)	Neoway Q7A	SIM868 (GNSS part)
Size (mm)	10.1 × 9.7 × 2.5	10.1 × 9.7 × 2.5	10.1 × 9.7 × 2.5	10.1 × 9.7 × 2.5	10.6 × 9.7 × 2.2	17.6 × 15.7 × 2.3
GPS	+	+	+	+	+	+
GLONASS	+	+	+	-	+	+
BeiDou	+	+	+	+	+	-
Galileo	+	+	+	-	-	-
QZSS	-	-	+	-	-	-
Sensitivity (dBm)	–167	–167	–165	~ –162	~ –162	~ –160
Cold start time (s)	~24	~26	~26	~32	~32	~30
Tracking current (mA)	~7	~23	~20	~25	~28	~25
Interfaces	UART, I²C, SPI	UART, I²C	UART, I²C	UART	UART	UART

B. Laboratory Bench Evaluation of GNSS Antenna Frequency Responses in a Shielded Anechoic Chamber

At the first stage of testing, the AFRs (S21) of four active ceramic antennas (1575R-A, Plosk, Uz, and Uzk) were investigated in the frequency range from 1.56 to 1.61 GHz. For comparative analysis, the commercial reference antenna u-blox W1220AS was used, with its response curve shown on each plot in Figure 6 for comparison. The measurements were conducted in the shielded AC of ISTT using a Keysight FieldFox vector network analyzer. Marker M1 indicates the GPS L1 frequency of 1.575 GHz, whereas marker M2 corresponds to 1.604 GHz (the midpoint of the GLONASS L1 band).

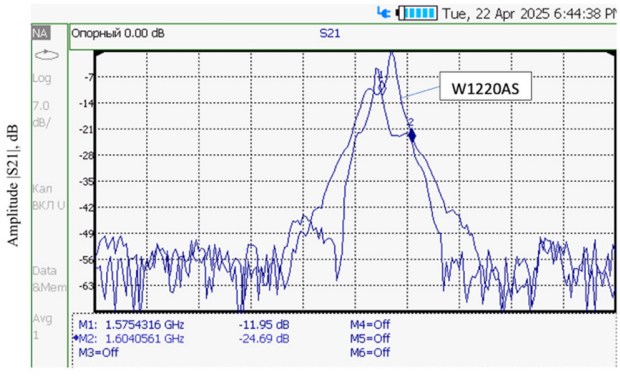

(a)

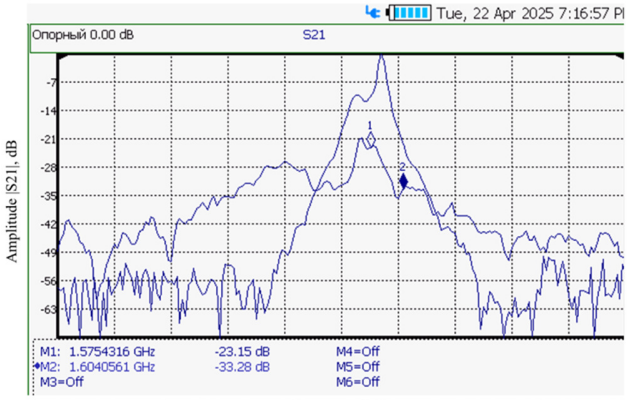

(b)

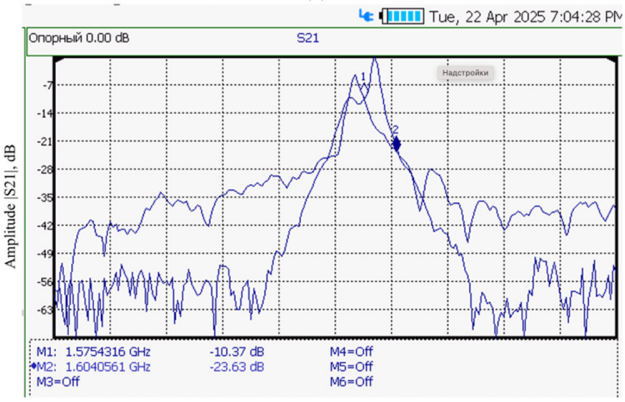

(c)

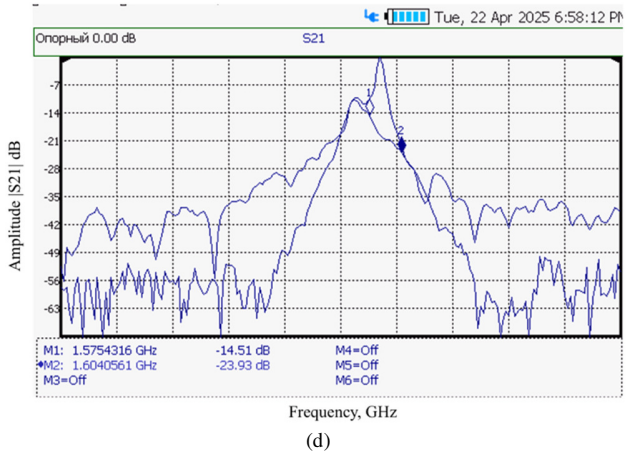

(d)

Fig. 6. AFRs of the tested antennas compared to the reference W1220AS antenna (upper trace without markers). M1 indicates the GPS L1 frequency, and M2 corresponds to the midpoint of the GLONASS L1 band: (a) 1575R-A antenna, (b) Plosk antenna, (c) Uz antenna, (d) Uzk antenna.

Figure 6(a) shows the measurement results of the 1575R-A antenna, with received signal levels of –11.95 dB at the GPS L1 frequency and –24.69 dB at the GLONASS L1 frequency. Figure 6(b) presents the Plosk antenna, with –23.15 dB at GPS L1 and –33.28 dB at GLONASS L1 frequency. The Uz antenna measurements are shown in Figure 6(c), with recorded levels of –10.37 dB and –23.63 dB, respectively. Figure 6(d) displays the Uzk antenna, which demonstrated –14.51 dB at GPS L1 and –23.93 dB at the GLONASS midpoint.

C. Field Tests Results of Receiver Performance within the Navigation Seal

At the second stage of testing, the reception characteristics of the antennas and modules were evaluated as part of a structural prototype of the developed navigation seal, mounted on a metal plate at a 45° angle to the horizon. The tests were carried out in open-field conditions and included measurements of cold-start time (TTFF), the number of visible satellites and those used in the solution, C/N₀ values for each satellite, as well as positioning accuracy parameters: PDOP, HDOP, and VDOP. These parameters reflect the geometric configuration of the satellites: PDOP characterizes the overall spatial quality of positioning, HDOP indicates horizontal coordinate accuracy (latitude and longitude), and VDOP refers to vertical positioning (altitude). Lower values of these coefficients indicate better positioning quality and more reliable satellite geometry.

Figure 7 shows the results of GNSS signal registration in open-field conditions, recorded using the Ublox GPS/GLONASS interface modified by specialists from the ISTT for integration into the developed ENS. Figure 7(a) presents data for navigation modules connected via COM10 and COM7 ports, whereas Figure 7(b) provides analogous results for modules connected through COM9 and COM6 ports. In each case, the recorded data include coordinates, FIX confirmation, the total number of visible satellites and those used in the solution, as well as C/N₀ values for each satellite. Satellites are identified by their Pseudo Random Noise (PRN) number, with the corresponding elevation angle (ELV), azimuth (AZ), and C/N₀ magnitude visualized through a graphical indicator.

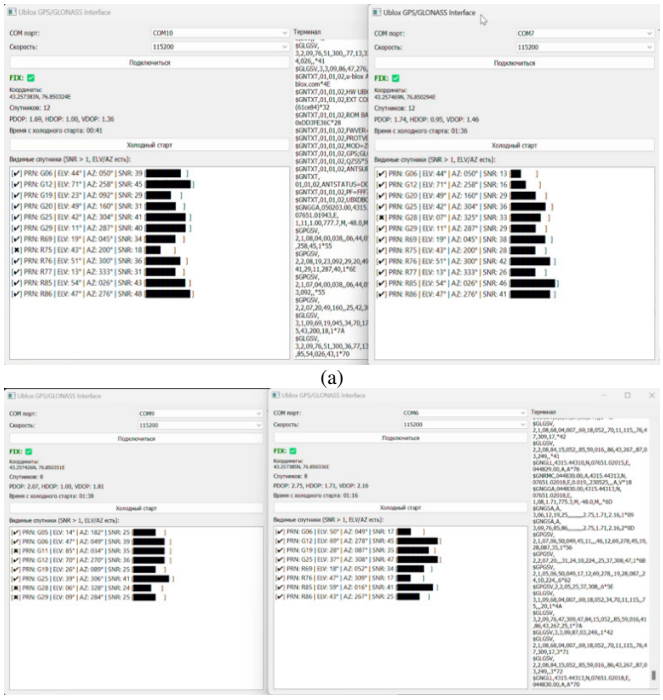

(a)

(b)

Fig. 7. GNSS signal reception results using the u-blox interface: (a) modules connected via COM10 and COM7 ports, and (b) modules connected via COM9 and COM6 ports.

The numerical data for cold-start time (TTFF), the number of visible satellites and those used in the solution, C/N₀ values, and geometry indicators (PDOP, HDOP, VDOP) are summarized in Table II.

TABLE II. FIELD TEST RESULTS OF NAVIGATION MODULE PERFORMANCE

Configuration	TTFF (s)	Number of satellites	C/N₀ (dB-Hz)	PDOP	HDOP	VDOP
COM10	41	12	48	1.69	1	1.36
COM7	96	12	46	1.74	0.95	1.46
COM9	98	8	41	2.07	1	1.81
COM6	76	8	47	2.75	1.71	2.16

The TTFF ranged from 41 to 98 s. The highest number of visible satellites was recorded for the COM7 configuration, with 12 satellites. The C/N₀ values per satellite ranged from 41 to 48 dB-Hz (minimum for COM9, maximum for COM10). The geometry indicators were as follows: PDOP 1.69–2.75, HDOP 0.95–1.71, and VDOP 1.36–2.16. All configurations successfully acquired positioning data during cold-start operation, with detailed results for each configuration summarized in Table II.

D. Results of Satellite Signal Reception

One of the key parameters determining the suitability of an antenna for practical use within a navigation seal is the cold-start TTFF, which characterizes the speed at which the receiver

acquires its first fixed position after being powered on. Table III summarizes the results of satellite signal registration using the 1575R-A antenna under open-field conditions and when installed inside the enclosure. The recorded values include cold-start time and C/N₀ levels for each satellite.

TABLE III. EXPERIMENTAL RESULTS OF SATELLITE SIGNAL RECEPTION FOR THE 1575R-A ANTENNA

Experiment	Cold start time		Satellite	C/N₀ (dB-Hz)	
	1575R-A	W1220AS		1575R-A	W1220AS
Open area (GPS + GLONASS)	0:41 (41 s)	1:16 (76 s)	G06	39	45
			G12	45	29
			G19	29	31
			G20	31	41
			G25	41	48
			G28	48	41
			G29	41	34
			R69	34	18
			R75	18	42
			R77	42	43
			R85	43	48
			R86	48	41
Enclosure installation (GPS only)	1:03 (63 s)	3:05 (185 s)	G29	46	44
			G20	44	43
			G25	38	43
			G06	37	37
			G05	30	30

When testing the 1575R-A antenna in open-field conditions, the average cold-start time was 41 s, whereas for the W1220AS antenna under the same conditions it was 76 s. During the experiment, signals from both GPS and GLONASS were recorded. The C/N₀ values for the 1575R-A antenna ranged from 18 to 48 dB-Hz, whereas for the W1220AS antenna they varied from 18 to 48 dB-Hz. When installed inside the enclosure, the 1575R-A antenna demonstrated a cold-start time of 63 s, compared to 185 s for the W1220AS. Despite the degraded conditions, the 1575R-A antenna maintained stable reception with C/N₀ values up to 46 dB-Hz. The total number of satellites registered in open-field conditions was 12.

In open-field conditions, the Plosk antenna demonstrated a cold-start time of 169 s, whereas the W1220AS achieved 54 s. For the Plosk antenna, the maximum recorded C/N₀ level was 42 dB-Hz. When installed inside the enclosure, the cold-start time was 149 s for the Plosk antenna and 213 s for the W1220AS. The highest C/N₀ values for the Plosk antenna were observed for satellites G25 and G20, 45 dB and 42 dB, respectively. Signal reception was absent for satellites G05, G20, G29, and R86. The total number of satellites detected in open-field conditions was 9. Table IV contains the test results for the Plosk antenna.

Table V presents the measured parameters for the Uz antenna, including cold-start time, the number of visible and used satellites, and the C/N₀ values for each satellite. Under open-field conditions, the Uz antenna achieved a cold-start time of 98 s, compared to 76 s for the reference W1220AS antenna. The maximum C/N₀ level for the Uz antenna was 47 dB-Hz, with a minimum of 17 dB-Hz. When installed inside the enclosure, the cold-start time increased to 115 s for the Uz antenna and 103 s for the W1220AS. Inside the enclosure, the signal levels for the Uz antenna ranged from 19 dB-Hz to 38 dB-Hz. The average number of registered satellites was 10.

TABLE IV. EXPERIMENTAL RESULTS OF SATELLITE SIGNAL RECEPTION FOR THE PLOSK ANTENNA

Experiment	Cold start time		Satellite	C/N₀ (dB-Hz)	
	Plosk	W1220AS		Plosk	W1220AS
Open area (GPS + GLONASS)	2:49 (169 s)	0:54 (54 s)	G05	39	45
			G06	45	29
			G12	29	31
			G20	31	41
			G25	41	48
			G29	48	41
			R69	41	34
			R70	34	18
			R75	18	42
			R76	42	43
			R86	43	48
Enclosure installation (GPS only)	2:29 (149 s)	3:33 (213 s)	G25	45	40
			G20	42	36
			G29	33	42
			G12	23	28

TABLE V. EXPERIMENTAL RESULTS OF SATELLITE SIGNAL RECEPTION FOR THE UZ ANTENNA

Experiment	Cold start time		Satellite	C/N₀ (dB-Hz)	
	Uz	W1220AS		Uz	W1220AS
Open area (GPS + GLONASS)	1:38 (98 s)	1:16 (76 s)	G05	25	-
			G06	39	17
			G11	35	-
			G12	36	45
			G19	25	35
			G25	41	47
			G28	24	-
			G29	25	-
			R69	-	34
			R76	-	17
			R85	-	41
			R86	-	25
Enclosure installation (GPS only)	1:55 (115 s)	1:43 (103 s)	G29	38	38
			G20	33	38
			G06	29	33
			G25	19	42

Table VI contains the test results for the Uzk antenna. In open-field conditions, the Uzk antenna achieved a cold-start time of 61 s, compared to 130 s for the reference W1220AS. Signal reception from GPS satellites was recorded with C/N₀ levels ranging from 11 dB-Hz to 39 dB-Hz. When installed inside the enclosure, the Uzk antenna demonstrated a cold-start time of 94 s, whereas the W1220AS achieved 46 s. Under enclosure conditions, the C/N₀ values for the Uzk antenna varied between 17 dB-Hz and 36 dB-Hz, whereas the W1220AS reached a maximum C/N₀ value of 47 dB-Hz. Up to 13 satellites were registered in open-field conditions.

Figure 8 presents a comparative summary of the cold-start times (TTFF) for the four tested antennas under two experimental scenarios: open-field conditions and installation inside the enclosure. The TTFF values were obtained during experimental trials conducted under identical conditions for all antennas. The minimum TTFF in open-field conditions was recorded for the 1575R-A antenna (41 s), whereas the maximum was observed for the Plosk antenna (169 s). Under

enclosure installation, the minimum start time was 63 s (1575R-A), and the maximum was 149 s (Plosk). The Uz antenna demonstrated TTFF values ranging from 98 s to 115 s, whereas the Uzk antenna ranged from 61 s to 94 s.

TABLE VI. EXPERIMENTAL RESULTS OF SATELLITE SIGNAL RECEPTION FOR THE UZK ANTENNA

Experiment	Cold start time		Satellite	C/N₀ (dB-Hz)	
	Uzk	W1220AS		Uzk	W1220AS
Open area (GPS + GLONASS)	1:01 (61 s)	2:10 (130 s)	G06	37	47
			G11	22	49
			G12	15	41
			G25	24	41
			G69	37	-
			G70	11	-
			G76	25	-
			G77	26	-
			G85	18	-
			G86	39	-
			G87	27	-
Enclosure installation (GPS only)	1:34 (94 s)	0:46 (46 s)	G29	36	43
			G12	34	33
			G20	27	34
			G25	21	47
			G19	17	18

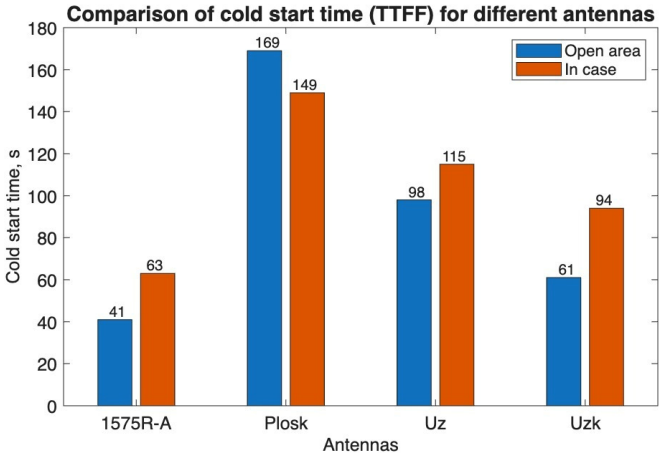

Fig. 8. Comparison of cold-start times (TTFF) for the four tested antennas under open-field conditions and within the enclosure installation.

The comparison showed that, for all antennas except Plosk, installation inside the enclosure resulted in an increase in cold-start time. The difference between the minimum and maximum TTFF values reached 128 s under open-field conditions and 86 s under enclosure installation. These results provide a quantitative assessment of the impact of structural design and installation conditions on the temporal performance of the antennas.

IV. DISCUSSION

In the course of the conducted experiments, a comprehensive evaluation of the performance of various GNSS antennas and modules was obtained when integrated into the developed navigation seal, intended for operation in the transport logistics environment of the Republic of Kazakhstan. The primary objective of this study was to select an antenna that is both cost-effective and operationally reliable, suitable for further implementation in the domestically developed navigation seal system. The findings address the central research question posed in this work: in the development of a locally manufactured navigation seal, designed in compliance with the requirements of the Decision of the Council of the Eurasian Economic Commission dated July 4, 2023, No. 75 [31], affordable commercial active antennas, when properly selected and preliminarily verified, are capable of providing reception characteristics comparable to those of imported industrial solutions. This opens up opportunities for the deployment of domestic production in the Republic of Kazakhstan, which is of strategic importance for Central Asian countries and the BRICS union in terms of technological independence and the strengthening of the national engineering and manufacturing base.

The comparative analysis of the four GNSS antenna types made it possible to identify the drawbacks of alternative solutions under conditions close to real-world operation. In particular, the Plosk antenna demonstrated the highest TTFF (169 s in open-field conditions), as well as the greatest sensitivity to the shielding effect of the enclosure. Moreover, the Plosk antenna showed a complete absence of signal reception from several satellites (G05, G20, G29, and R86).

The Uz and Uzk antennas, which occupied intermediate positions in terms of performance, exhibited a significant increase in TTFF when installed inside the enclosure. The TTFF for the Uz antenna increased to 115 s (from 98 s), whereas for the Uzk antenna it increased to 94 s (from 61 s). These results contrast with the performance of the 1575R-A antenna, which ensured the lowest TTFF and demonstrated the least degradation in performance when mounted inside the enclosure (63 s).

The measurement analysis reveals a consistent pattern. The 1575R-A antenna demonstrated the shortest TTFF and the least sensitivity to installation conditions. In both open-field and enclosure scenarios, it maintained high C/N₀ (dB-Hz) values and a stable number of tracked satellites, making it a practical candidate for large-scale implementation in domestic ENSs.

In our experiments, the installation of antennas on metallic surfaces resulted in a reduction of C/N₀ and an increase in TTFF. These observations are consistent with the findings reported in [18], which demonstrated that the presence of objects in the near-field region of GNSS antennas alters their electromagnetic characteristics, leading to increased variance and systematic biases (up to ~3 mm in the Up component) in Precise Point Positioning (PPP) solutions. This effect was shown to be more pronounced during short observation sessions and for large choke-ring antennas. The experimental results demonstrate that the S21 parameter should not be considered as the sole reliable criterion for antenna selection. Rather, it is a parameter useful for monitoring the frequency response during incoming component inspection, maintenance, or repair. Discrepancies between laboratory and field measurements are common in practice, particularly when the specific design (form factor) and antenna integration, combined with surrounding conductive surfaces, wiring, and enclosure materials, may distort the radiation pattern, polarization, phase

center, or VSWR. This is especially typical for compact or electrically shortened antennas, whose near-field region is effectively "compressed" relative to the wavelength and strongly influenced by the dielectric constant of the ceramic material. Under "on-metal" installation conditions, not all performance aspects can be predicted solely based on the S21 parameter. Moreover, multipath modeling that accounts for reflections from metallic surfaces demonstrates that when the gap between the antenna's phase center and the conducting plane is small, the period of multipath error increases sharply, leading to systematic biases in PPP solutions [19].

The results of the conducted tests showed that the 1575R-A antenna is the most well-balanced solution in terms of overall performance. It demonstrated the shortest cold-start time, stable C/N₀ values, and low sensitivity to installation conditions. The technical specifications of the GNSS 1575R-A antenna are presented in Table VII. Thus, it has been established that the 1575R-A antenna demonstrates the most optimal characteristics among the tested samples and can be recommended for integration into the developed navigation seal.

TABLE VII. TECHNICAL SPECIFICATIONS OF THE 1575R-A ANTENNA

Parameter	Nominal value
Receiving frequency range (MHz)	1575.42 ± 1.023
Center frequency (-10dB bandwidth) (MHz)	1575 ± 3.0
VSWR at center frequency	1.5
Gain (zenith 90o) (dBic)	4.3
Impedance (Ω)	50 ± 10
Polarization model	RHCP
Frequency temperature coefficient (ppm/oC)	20

The practical significance of this work lies in the fact that, for the first time in the Republic of Kazakhstan, it demonstrates a functional approach to the comprehensive experimental evaluation of GNSS antennas for navigation seals, taking into account real operating conditions typical of national logistics routes and digital customs control tasks. The recommendations obtained make it possible to enhance Kazakhstan's technological independence in the development and large-scale implementation of domestic cargo monitoring systems, while simultaneously reducing costs through the justified selection of optimal components. This directly supports import-substitution initiatives, the development of the local engineering school, and the advancement of Kazakhstan's digital logistics infrastructure.

The theoretical significance of this work lies in deepening the understanding of how design and operational factors affect the performance of GNSS antennas in compact electronic devices. The results of this study expand the empirical database, complementing existing theoretical models of antenna interaction with the enclosure and the surrounding electromagnetic environment. This is important for further optimization of such systems not only in the Republic of Kazakhstan but also in countries facing similar tasks and operating conditions.

The limitations of this study include testing only a limited set of antennas and the absence of experiments under extreme climatic conditions. In addition, no long-term evaluation of the operational stability of the navigation seal was performed. Future research should focus on expanding the range of tested solutions and analyzing the resilience of such systems to seasonal and climatic influences. Thus, this study has not only identified the optimal antenna in terms of both cost-effectiveness and performance characteristics but has also established a scientific and practical foundation for the further implementation of the selected solution in domestically developed ENSs. This is particularly significant for advancing intelligent transportation systems and strengthening the logistics infrastructure of the Republic of Kazakhstan.

V. CONCLUSIONS

In this study, a comprehensive experimental evaluation of the performance of cost-effective Global Navigation Satellite System (GNSS) antennas and modules integrated into Electronic Navigation Seals (ENSs) intended for transport logistics in the Republic of Kazakhstan was conducted. The analysis of the test results demonstrated that certain commercial antennas, particularly the 1575R-A model, are capable of delivering reception parameters comparable to industrial-grade solutions, provided that they are properly selected and positioned within the device. It was shown that the most critical factors affecting signal reception efficiency are the structural design of the antennas and the conditions of their installation.

The obtained results confirm the proposed hypothesis regarding the feasibility of using antennas optimized in terms of both cost and performance for subsequent integration into domestically developed ENSs. This finding opens up prospects for the creation and large-scale deployment of modern, economically efficient monitoring systems that fully comply with the requirements of digital logistics and customs control in the Republic of Kazakhstan.

The practical significance of this study lies in the development of scientifically grounded recommendations for local manufacturers on the selection and testing of antennas under conditions closely approximating real-world operation. The theoretical significance lies in the advancement of understanding regarding the impact of operational factors on the performance of GNSS antennas in compact devices, as well as in the enrichment of existing engineering methodologies with new empirical data. Thus, the results of this study not only allow the recommendation of specific antennas for integration into domestically developed ENSs, but also provide a scientific and practical foundation for the further advancement of intelligent transport systems and logistics infrastructure both in the Republic of Kazakhstan and in other Central Asian countries, as well as in BRICS member states.

In the future, comprehensive testing of the developed navigation seal as part of a fully assembled device is planned, with the purpose of evaluating the interaction of all subsystems, including satellite modules, the controller, and the power supply system. The tests will focus on assessing positioning accuracy, coordinate stability, energy efficiency, and data transmission reliability under various operational scenarios.

In addition, a series of field and climatic tests is planned across different climate zones of Kazakhstan, including exposure to extreme temperatures, high humidity, dust, and vibrations. This will allow for evaluation of the operational robustness of the navigation seal and antenna under seasonal changes and long-term use, as well as refinement of the structural and software requirements for mass production.

ACKNOWLEDGMENT

This research was funded by the Committee of Science of the Ministry of Science and Higher Education of the Republic of Kazakhstan (Grant No. BR24992884 "Development of a prototype of an electronic identifier in order to further organize their production").

REFERENCES

[1] *Freight containers — Electronic seals, Part 1: Communication protocol*, ISO 18185-1, 2007.

[2] *Freight containers — Electronic seals, Part 3: Environmental characteristics*, ISO 18185-3, 2015.

[3] *Freight containers — Electronic seals, Part 4: Data protection*, ISO 18185-4, 2007.

[4] A. Leick, L. Rapoport, and D. Tatarnikov, *GPS Satellite Surveying*, 4th ed. Hoboken, NJ, USA: John Wiley & Sons, 2015.

[5] P. J. G. Teunissen and O. Montenbruck, *Springer Handbook of Global Navigation Satellite Systems*, Cham, Switzerland: Springer International Publishing, 2017, https://doi.org/10.1007/978-3-319-42928-1.

[6] V. Hamza, B. Stopar, O. Sterle, and P. Pavlovčič-Prešeren, "Observations and positioning quality of low-cost GNSS receivers: a review," *GPS Solutions*, vol. 28, no. 3, June 2024, Art. no. 149, https://doi.org/10.1007/s10291-024-01686-8.

[7] V. Hamza, B. Stopar, O. Sterle, and P. Pavlovčič-Prešeren, "Recent advances and applications of low-cost GNSS receivers: a review," *GPS Solutions*, vol. 29, no. 1, Jan. 2025, Art. no. 56, https://doi.org/10.1007/s10291-025-01815-x.

[8] S. R. Best, "The Significance of Ground-Plane Size and Antenna Location in Establishing the Performance of Ground-Plane-Dependent Antennas," *IEEE Antennas and Propagation Magazine*, vol. 51, no. 6, pp. 29–43, Dec. 2009, https://doi.org/10.1109/MAP.2009.5433095.

[9] S. Punzet and T. F. Eibert, "Impact of Additional Antenna Groundplanes on RTK-GNSS Positioning Accuracy of UAVs," *Advances in Radio Science*, vol. 20, pp. 23–28, Mar. 2023, https://doi.org/10.5194/ars-20-23-2023.

[10] Taoglas, *Internal GPS Active Patch Antenna Application Note*. San Diego, CA, USA: Taoglas, 2018.

[11] I. Broumas, "Design of Cellular and GNSS Antenna for IoT Edge Device," M.S. thesis, School of Information Technology, Halmstad University, Halmstad, Sweden, 2019.

[12] Z. Liu *et al.*, "A local filtering approach to mitigating the GNSS multipath effects in relative precise positioning considering the multipath spatial correlation," *Advances in Space Research*, vol. 74, no. 6, pp. 2709–2727, Sept. 2024, https://doi.org/10.1016/j.asr.2024.03.017.

[13] N. Vagle, A. Broumandan, A. Jafarnia-Jahromi, and G. Lachapelle, "Performance analysis of GNSS multipath mitigation using antenna arrays," *The Journal of Global Positioning Systems*, vol. 14, no. 1, Nov. 2016, Art. no. 4, https://doi.org/10.1186/s41445-016-0004-6.

[14] Z. Xue, Z. Lu, Z. Xiao, J. Song, and S. Ni, "Overview of multipath mitigation technology in global navigation satellite system," *Frontiers in Physics*, vol. 10, Dec. 2022, Art. no. 1071539, https://doi.org/10.3389/fphy.2022.1071539.

[15] S. Pawar, D. Lee, H. Skinner, S.-Y. Suh, and A. Yakovlev, "Decoupling and Cloaking of Rectangular and Circular Patch Antennas and Interleaved Antenna Arrays with Planar Coated Metasurfaces at C-Band Frequencies—Design and Simulation Study," *Sensors*, vol. 24, no. 1, Jan. 2024, Art. no. 291, https://doi.org/10.3390/s24010291.

[16] K. C. Rao *et al.*, "An Integrated Dual Antenna for Multi-Band Satellite Communication Applications," *Engineering, Technology & Applied Science Research*, vol. 15, no. 3, pp. 23707–23713, June 2025, https://doi.org/10.48084/etasr.10372.

[17] A. Dave, R. Saborio, K. Sun, R. Sainati, D. Gebre-Egziaher, and R. Franklin, "Characterizing Phase-Center Motion of GNSS Antennas Used in High-Accuracy Positioning," Center for Transportation Studies, University of Minnesota, CTS Report 19-17, June 2019.

[18] P. Hillyard, C. Qi, A. Al-Husseiny, G. D. Durgin, and N. Patwari, "Focusing through walls: An E-shaped patch antenna improves whole-home radio tomography," in *2017 IEEE International Conference on RFID*, Phoenix, AZ, USA, 2017, pp. 174–181, https://doi.org/10.1109/RFID.2017.7945605.

[19] K. Dawidowicz and R. Baryła, "GNSS Antenna Caused Near-Field Interference Effect in Precise Point Positioning Results," *Artificial Satellites*, vol. 52, no. 2, pp. 27–40, June 2017, https://doi.org/10.1515/arsa-2017-0004.

[20] F. Dilssner, G. Seeber, G. Wübbena, and M. Schmitz, "Impact of Near-Field Effects on the GNSS Position Solution," in *Proceedings of the 21st International Technical Meeting of the Satellite Division of The Institute of Navigation*, Savannah, GA, USA, 2008, pp. 612–624.

[21] M. Anghileri, M. Paonni, S. Wallner, J.-A. Avila-Rodriguez, and B. Eissfeller, "Estimating the Time-To-First-Fix for GNSS Signals Theory and Simulation Results," in *Proceedings of the European Navigation Conference*, Toulouse, France, 2008.

[22] J. Jang, D. Park, S. Sung, and Y. J. Lee, "HDOP and VDOP Analysis in an Ideal Placement Environment for Dual GNSSs," *Sensors*, vol. 22, no. 9, May 2022, Art. no. 3475, https://doi.org/10.3390/s22093475.

[23] M. Specht, "Experimental studies on the relationship between HDOP and position error in the GPS system," *Metrology and Measurement Systems*, vol. 29, no. 1, pp. 17–36, Mar. 2022, https://doi.org/10.24425/mms.2022.138549.

[24] R. Blay, B. Wang, and D. M. Akos, "Deriving Accurate Time from Assisted GNSS Using Extended Ambiguity Resolution," *Navigation: Journal of the Institute of Navigation*, vol. 68, no. 1, pp. 217–229, Mar. 2021, https://doi.org/10.1002/navi.412.

[25] C. Hernando-Ramiro, Ó. Gamallo-Palomares, J. Junquera-Sánchez, and J. A. Gómez-Sánchez, "Time to First Fix Robustness of Global Navigation Satellite Systems: Comparison Study," *Sensors*, vol. 25, no. 5, Mar. 2025, Art. no. 1599, https://doi.org/10.3390/s25051599.

[26] *MAX-M10S Integration Manual*, 4th ed., u-blox AG, Thalwil-Zürich, Switzerland, 2023.

[27] "MAX-M10 series." u-blox. https://www.u-blox.com/en/product/max-m10-series.

[28] "MAX-8 series." u-blox. https://www.u-blox.com/en/product/max-8-series.

[29] B. Medetov, A. Kulakayeva, A. Zhetpisbayeva, N. Albanbay, and T. Kabduali, "Identifying the regularities of the signal detection method using the Kalman filter," *Eastern-European Journal of Enterprise Technologies*, vol. 5, no. 9 (125), pp. 26–34, Oct. 2023, https://doi.org/10.15587/1729-4061.2023.289472.

[30] V. Tikhvinskiy, A. Pastukh, S. Dymkova, and O. Varlamov, "Compatibility Analysis Between RedCap Non-Public Networks and 5G NR in TDD FR1 and FR2 Bands," *Inventions*, vol. 10, no. 1, Feb. 2025, Art. no. 12, https://doi.org/10.3390/inventions10010012.

[31] "Decision of Council of the Eurasian economic commission of July 4, 2023 No. 75: About requirements to the navigation seals applied when transporting goods on the territories of two and more state members of Eurasian economic." Cis-legislation. https://cis-legislation.com/document.fwx?rgn=151988.